Radiotherapy and Oncology 191 (2024) 110087

Contents lists available at ScienceDirect

Radiotherapy and Oncology

journal homepage: www.thegreenjournal.com

Original Article

Intratumor genetic heterogeneity and head and neck cancer relapse

A.S. Pierik [a,b], J.B. Poell [a,b], A. Brink [a,b], M. Stigter- van Walsum [a,b], R.H. de Roest [a,b], T. Poli [c], A. Yaromin [d], P. Lambin [d], C.R. Leemans [a], R.H. Brakenhoff [a,b,*]

[a] Amsterdam UMC location Vrije Universiteit Amsterdam, Department of Otolaryngology/Head and Neck Surgery, Head and Neck Cancer Biology and Immunology laboratory, De Boelelaan 1117, Amsterdam, the Netherlands
[b] Cancer Center Amsterdam, Cancer Biology and Immunology, De Boelelaan 1117, Amsterdam, the Netherlands
[c] Maxillofacial Surgery Unit, Department of Medicine and Surgery - University of Parma, University Hospital of Parma, Via Gramsci 14, Parma, Italy
[d] Maastricht University, Department of Precision Medicine-UM & Radiology-MUMC, Universiteitssingel 40, Maastricht, the Netherlands

ARTICLE INFO

Keywords:
Itratumor genetic heterogeneity
Recurrence
Head and neck cancer
HNSCC
ITGH

ABSTRACT

Background: Head and neck squamous cell carcinomas are treated by surgery, radiotherapy (RT), chemoradiotherapy (CRT) or combinations thereof, but locoregional recurrences (LRs) occur in 30–40% of treated patients. We have previously shown that in approximately half of the LRs after CRT, cancer driver mutations are not shared with the index tumor.
Aim: To investigate two possible explanations for these genetically unrelated relapses, treatment-induced genetic changes and intratumor genetic heterogeneity.
Methods: To investigate treatment-induced clonal DNA changes, we compared copy number alterations (CNAs) and mutations between primary and recurrent xenografted tumors after treatment with (C)RT. Intratumor genetic heterogeneity was studied by multi-region sequencing on DNA from 31 biopsies of 11 surgically treated tumors.
Results: Induction of clonal DNA changes by (C)RT was not observed in the xenograft models. Multi-region sequencing demonstrated variations in CNA profiles between paired biopsies of individual tumors, with copy number heterogeneity scores varying from 0.027 to 0.333. In total, 32 cancer driver mutations could be identified and were shared in all biopsies of each tumor. Remarkably, multi-clonal mutations in these same cancer driver genes were observed in 6 of 11 tumors. Genetically distinct heterogeneous cell cultures could also be established from single tumors, with different biomarker profiles and drug sensitivities.
Conclusion: Intratumor genetic heterogeneity at the level of the cancer driver mutations might explain the discordant mutational profiles in LRs after CRT, while there are no indications in xenograft models that these changes are induced by CRT.

Introduction

Head and neck squamous cell carcinoma (HNSCC) develops in the epithelial cells of the mucosal lining of the upper aerodigestive tract. HNSCC is one of the more common cancers with approximately 900,000 new cases per year diagnosed worldwide [1,2]. Exogenous carcinogens such as tobacco and alcohol are the classic risk factors for HNSCC. More recently a persistent infection with the human papillomavirus (HPV) has been recognized as risk factor [3], particularly in oropharyngeal squamous cell carcinomas (OPSCC). HPV-positive OPSCC have a more favorable prognosis, a different molecular profile, and are considered a separate disease entity as compared to HPV-negative OPSCC [4].

Treatment for cure of HNSCC depends on site, stage of the disease, histological findings after surgery, and physical condition including age of the patient. For advanced stage tumors (III–IV) outside the oral cavity definitive chemoradiotherapy (CRT) is applied, the concomitant

Abbreviations: CNA, Copy number alteration; CNH, Copy number heterogeneity; CRT, Chemoradiotherapy; DCS, Duplex consensus sequencing; DMEM, Dulbecco's Modified Eagle's Medium; DNA, Deoxyribonucleic acid; FBS, fetal bovine serum; FFPE, Formalin-fixed paraffin-embedded; Gy, Gray; HPV, Human papillomavirus; IGV, Integrative Genomics Viewer; lcWGS, low coverage whole genome sequencing; PCR, Polymerase chain reaction; PT, Primary tumor; RT, Radiotherapy; SNPs, Single nucleotide polymorphisms; SPT(s), Second primary tumor(s); VAF, Variant allele frequency.

* Corresponding author at: Department of Otolaryngology / Head & Neck Surgery, Location VUmc, De Boelelaan 1117 1081 HV, Amsterdam.
E-mail address: rh.brakenhoff@amsterdamumc.nl (R.H. Brakenhoff).

https://doi.org/10.1016/j.radonc.2024.110087
Received 2 August 2023; Received in revised form 18 December 2023; Accepted 3 January 2024
Available online 6 January 2024

application of systemic cisplatin-based chemotherapy and locoregional RT. Advanced stage oral cancers are generally treated with a combination of surgery and postoperative RT with or without chemotherapy [3].

Despite substantial advances in imaging, diagnostics, and treatment options for patients with head and neck squamous cell carcinoma (HNSCC), the 5-year overall survival (OS) has only modestly improved last few decades, and these figures may be even overvalued by the increasing fraction of HPV-positive OPSCC with more favorable prognosis. The major clinical problem are still local recurrences (LRs). LRs are clinically defined as a recurrent tumor within 2 cm of the primary tumor and within 3 years after first diagnosis[5]. LRs develop in 30–40 % of advanced stage HPV-negative patients, and are difficult to manage as they are mostly detected late [6,7].

The origin of LRs has been widely studied especially in surgically treated patients. LRs after surgery can be explained by residual tumor cells and alternatively by field cancerization [8–11]. In a few recent studies the pathobiological origin of LRs after (C)RT has been investigated. De Roest et al. studied the genetic relationships of primary tumors (PTs) and LRs of patients treated with CRT[12], and showed by copy number alteration (CNA) profiling and mutational analysis of the most frequently mutated cancer driver genes, that only half of the relapses appeared to be genetically related to the corresponding PTs, while the other half seemed genetically unrelated. Hedberg et al. reported data from a similar study but noted absence of genetic relationships in 1 of 10 studied pairs[8]. Most recently, Weber et al. studied a cohort of samples of tumors and LRs treated by surgery with or without adjuvant (C)RT or definitive (C)RT and demonstrated that 15 % was not genetically related based on the mutational profile[13]. In the latter study patients were treated with a mix of modalities, which makes extrapolation of results difficult.

Despite the differences in reported frequencies: in all studies a subgroup of LRs appeared to be genetically unrelated to the PT after (C)RT varying from 10 % to 50 %. There are multiple explanations for these findings. Field cancerization might play a role, as has been reported for surgically treated patients, but seems less likely as this implies sharing of at least some genetic changes, while in these seemingly genetically unrelated LRs after CRT no changes at all were shared. Definitive (C)RT might also have induced genetic changes. It has been well established that RT and cisplatin cause specific mutational signatures [14,15]. It is therefore well conceivable that LRs after (C)RT may have acquired additional mutations, although this would not explain the observation that driver mutations present in the index tumors seemed to have disappeared in LRs.

Another explanation might be that tumors are genetically heterogeneous and contain different clones with distinct mutations, and some of these clones characterized by different driver mutations might be selected for outgrowth by the treatment. This intratumor genetic heterogeneity has been well studied in other tumor models mostly by exome sequencing, but generally most cancer driver genes were shared [16–18]. Here we studied both treatment induction of mutations in animal models, and heterogeneity at the level of the cancer driver genes, as possible explanations for these seemingly genetically unrelated LRs after CRT.

Methods

Animal models

Xenograft models are described in the Supplementary methods.

Multi-region biopsies

Patients with a primary tumor surgically treated at Amsterdam UMC or the University Hospital of Parma were enrolled. Spatially distinct biopsies were taken from the resection specimen after surgery, aiming at 3 biopsies per patient. In total, 31 biopsies from 11 resected primary tumors were collected and analyzed. Caution was taken to have sufficient spatial distance between the biopsies. None of the patients received treatment before surgery. Biopsies were snap-frozen and stored in liquid nitrogen. The study was approved by the Institutional Review Boards of Amsterdam UMC and Parma University Hospital, and was carried out according to the Federa guidelines on studies with human tissues and the privacy act of the EU commission.

Heterogeneous cell cultures of tumor biopsies

Biopsies were collected in storage medium (DMEM with 5 % fetal bovine serum (FBS), gentamicin 5 mg/ml Amphotericin B 2.50 μg/ml) and incubated overnight at 4 °C. Next day, biopsies were cut in small pieces and plated in Matrigel in several wells in DMEM/F12 with 5 % FBS and Primocin antibiotics (InvivoGen). Cultures that proliferated well were inspected for cells with different morphology, and morphologically different cell clones were selected by differential trypsinization when possible. Cultures were genetically characterized as described below, immunohistochemical biomarkers as well as drug sensitivity were evaluated according to van Harten et al.[19]. The study was approved by the Institutional Review Board at Amsterdam UMC and patients were enrolled in the study after written informed consent.

Sequencing and data analysis

Samples workup, sequencing and data analysis is described in the Supplementary methods.

Copy number heterogeneity score of multi-region biopsies

For each patient, one of the biopsy samples (generally with highest purity) was designated as anchor sample, and tumor purity and ploidy for this sample was determined using ACE, finding the best fit in terms of both copy numbers and mutant copies of driver mutations. Concordant fits were determined for all other biopsy samples of the patient by minimizing the summed distance of the segments to both the nearest integer and the corresponding segments of the anchor fit. The multisample Copy Number Heterogeneity score (CNH-score) was calculated as the copy number standard deviation (sd) of all paired samples, calculated over all segments (i), and weighted by segment length (w): $\frac{\sum w(i)sd(i)}{\sum w(i)}$. The method of calculating the multisample CNH-score is also displayed in Supplementary Fig. 1.

Clonality analysis of mutations in multiregion biopsies

To ensure accurate (sub)clonal mutation calling we performed duplex consensus sequencing (DCS) analysis with a cut-off of > 3 DCS reads [20]. By DCS analysis, sequencing artefacts are removed, and at this level of > 3 DCS reads rare somatic mutations are also discarded, and reliable (sub) clonal mutations remain. Variant copies were calculated based on the VAF, the copy number of that locus, and tumor purity using the linkvariants function of the ACE package. Somatic mutations were defined as clonal when they were present with more than or equal to 0.5 copies in the tumor cells, based on the assumption that a cancer driver gene can be mutated on one allele. We defined a mutation as subclonal if it was present with fewer than 0.5 copies but above background. The significance above background was calculated by a Poisson test on the VAFs, and only considered when the VAF was significantly higher ($P < 0.001$) than the VAF of all other samples of all patients at that position. A unique variant was defined as a clonal or a subclonal variant present in only one biopsy but not in any other biopsy of the same tumor as calculated above. Variant copy rate ratios and associated p-values are calculated using the R stats poisson.test function comparing the rates of variant-supporting reads with other samples in the same tumor, corrected for the sample tumor purity. Code is available on request.

Results

In the VU-SCC-OE xenograft model that responds to 2x 3 mg/kg cisplatin and 2x 2 Gy RT (Fig. 1), we did not note any clonal change in mutations or CNA-profiles that was induced by the treatment (data not shown). However, this model is more a residual disease than recurrence model, and RT doses are much lower than used in patients.

The FaDu model is a more realistic HNSCC relapse model. The 2 untreated tumors were collected after 1–2 weeks after tumor cell injection, and growth curves are shown in Supplementary Fig. 2 and Fig. 3. For the two treated xenografts that were sequenced, one tumor received 50 Gy, 1.66 Gy/fx daily for 6 weeks and the LR was collected at day 47 following the last radiation fraction, while the second tumor received 60 Gy (2 Gy/fx, 30 fx) and the LR was collected at day 52 after the last RT treatment. These tumors were strongly reduced in size by the high dose radiotherapy and needed almost two months to recur. Both lcWGS and target-enrichment sequencing were performed on the DNA of the primary xenograft and the relapsed tumors. We noted small differences in the CNA profiles, but these did not relate to the treatment (Supplementary Figs. 3–7). Key driver mutations known to be present in FaDu cells in *TP53, KDM6A, CDKN2A* and *FAT1* were present in the recurrence. Additional mutations were only found at low VAF and equally distributed over treated and untreated tumors. Obviously we tested a limited number of samples and cell lines, but the complete lack of any induced clonal mutation in the driver genes in both cell line models, indicated that this seems a not very convincing explanation of these seemingly unrelated recurrences after CRT.

Next, we investigated whether intratumor genetic heterogeneity could serve as an alternative explanation for the discordant driver mutations between primary and recurrent tumors.We collected biopsies from multiple regions of resected tumors, and analyzed presence of multiclonal mutations in the cancer driver genes. In total, 31 spatially distinct biopsies were studied from 11 cancer specimen after surgery, with a median of 3 biopsies per patient. Patient characteristics are listed in Table 1.

Both low coverage whole genome sequencing was performed to generate copy number profiles and target-enrichment sequencing for mutations. Copy number profiles and mutational data were used to determine both ploidy and cellularity (tumor percentage) of individual biopsies based on the most likely fit across all samples of a tumor. The tumor percentage of biopsy 3 from tumor ITGH-6 was below 5 % and therefore excluded from further analysis.

The copy number profiles showed the characteristic alterations for HNSCC with losses and gains at 3p, 8p, 9p, and 11q. Most CNAs were identical between biopsies of the same tumor, but differences between biopsies were observed to varying degrees in all tumors. This is exemplified in patient ITGH-15; two biopsies share several CNAs with specific breakpoints (e.g. on chromosome 3 and 9), but both also harbor unique CNAs (Fig. 2A). To quantify copy number heterogeneity we developed a multisample CNH-score defined as the standard deviation of segments between paired samples averaged across the genome (Supplementary Fig. 1). Multisample CNH-scores ranged from 0.027 to 0.333 across all patients (Fig. 2B). We further noted a good correlation between our multiregion CNH-score and the single biopsy CNH-score by van Dijk et al. (Fig. 2C)(21).

We next analyzed intratumoral genetic heterogeneity at the level of the driver gene mutations. For mutation calling, target-enrichment sequencing was performed using a capture panel that included 29 human cancer driver genes frequently altered in HNSCC according to the data from TCGA, supplemented with full genome of HPV 16 and E7 sequences of 14 other high risk HPV types (Supplementary Table 1 + [22]), and sequenced these with high coverage. Mean coverage of all samples was 4,178 (range 1,973 – 5,794) (see Supplementary Table 2 for detailed coverage information). No HPV reads of significance were found in our analysis as expected for oral cancers. All called variants are listed in Supplementary Table 3.

The median number of variants per tumor was 3 (range 1–7). All biopsies of every tumor shared the clonal driver mutations. However, 6 of 11 tumors showed multiple subclonal driver mutations in one or more biopsies. Subclonal mutations were also found in the well-known driver

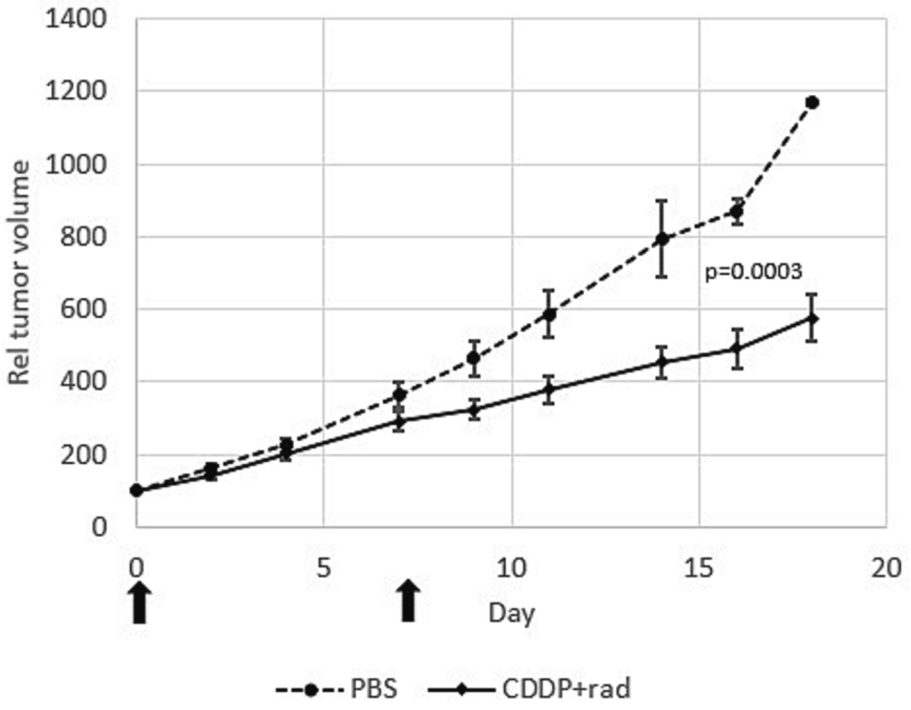

Fig. 1. Response of VU-SCC-OE xenografts on CRT. Relative tumor volumes with standard error of the mean are depicted (8 mice per group). At day 0 and day 8, 3 mg/kg CDDP and 2 Gy radiation was administered (indicated with black arrows). At day 16 (the last day that all mice remained in the study), the tumor volume in the treated group was significantly smaller compared to the untreated group (P = 0.003, 2-tailed Mann-Whitney *U* test).

Table 1
Patient characteristics.

Study ID	Gender	Age diagnosis	Alcohol(units per week)	Smoking (pack years)	Subsite	TNM Stage	#biopsies
ITGH-3	M	68	6	56	Floor of mouth	pT1N0	3
ITGH-4	M	80	missing	20	Retromolar trigone	pT4aN2b	3
ITGH-5	M	64	28	40	Retromolar trigone	pT4aN0	3
ITGH-6	M	69	7	12	Retromolar trigone	pT4aN2b	2
ITGH-7	M	67	30	13	Retromolar trigone	pT4aN1	5
ITGH-10	F	53	35	30	Floor of mouth	pT4aN2c	3
ITGH-13	M	82	14	<5	Palate	pT4aN0R1	2
ITGH-14	M	62	40	22	Cheek	pT4aN0	3
ITGH-15	F	72	<1	0	Lower alveolar ridge	pT4aN2b	3
NPR206	M	86	0	0	Cheek	pT2N2b	2
NPR207	M	58	0	0	Retromolar trigone	pT4N1	2
HN937	M	73	34	6	Larynx	pT4aN1	2

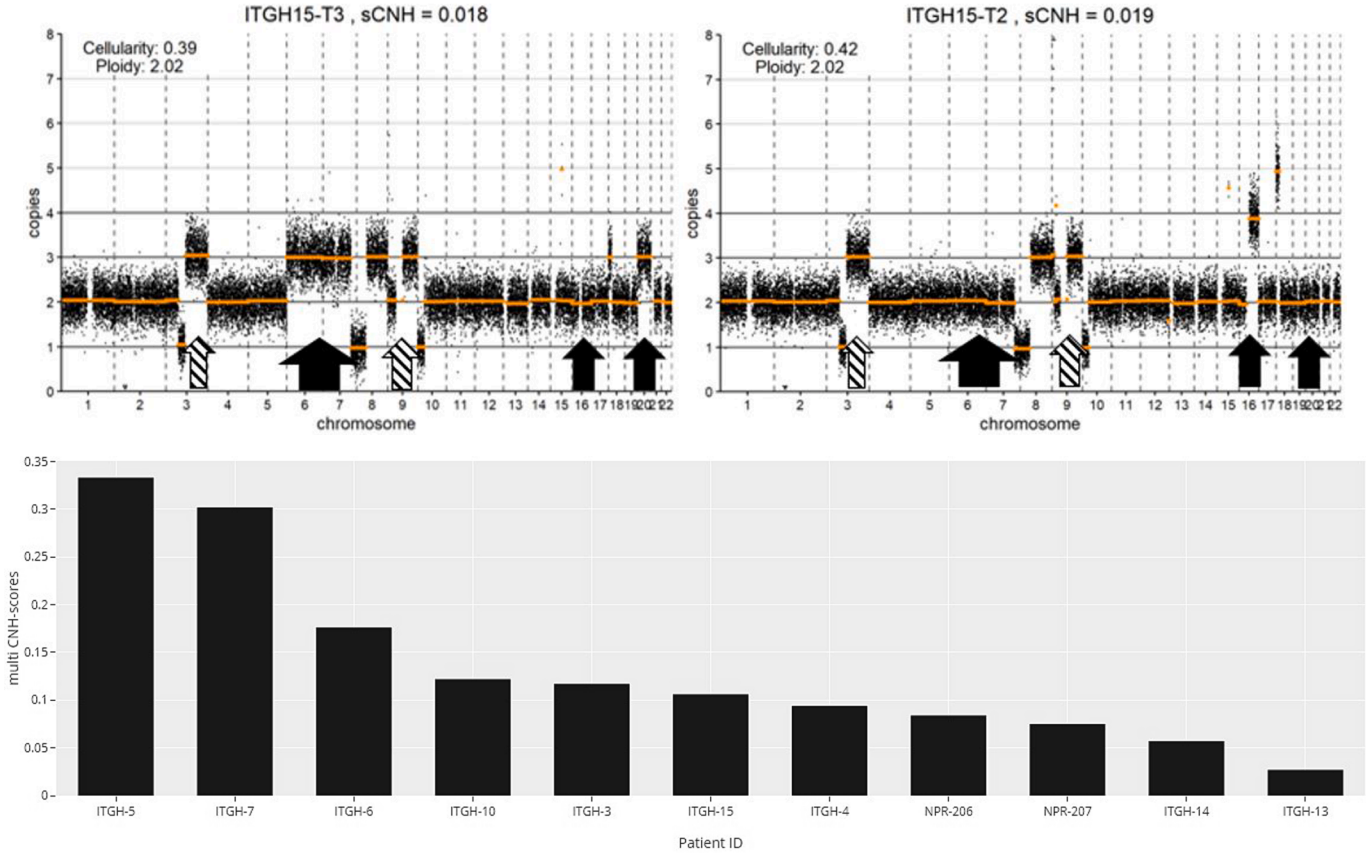

Fig. 2. A). Intratumor genetic heterogeneity by multiregion sequencing. The copy number profiles of biopsy T2 and T3 of tumor ITGH-15 are depicted: some differences are indicated with a closed arrow and some similarities are indicated with a striped arrow. B). Waterfall plot of the calculated **m**ultiregion-CNH-Scores. C). Correlation plot of the multiregion CNH-score and the single CNH score according to (21) R^2 = 0.942, p < 0.0001.

genes *TP53* and *PIK3CA*, already by standard analysis pipelines. DCS analysis, which is very specific by combining the variant data of the complementary DNA strands and allowing specific mutation detection at much lower VAF, revealed 3 extra variants in driver genes displayed in Fig. 3. An interesting case is ITGH-7 since clonal mutations occurred in *CDK2NA* (c.387C > A; p.Y129*), KMT2D (c.16373A > T; p.E5458V) and *TP53* (c.811G > A; p.E271K) in all 5 biopsies, but an extra *TP53* subclonal mutation (c.320A > G; p.Y107C) was present in the second biopsy only. This *TP53* mutation was absent in all other biopsies (0 variant base calls with coverage between 554 and 1,614) while it was convincingly present with 29 DCS reads with a coverage of 1,005 in that particular biopsy. Additionally, a subclonal *PIK3CA* mutation (c.3140A > G; p.H1047R) was detected in biopsy 4 with 10 DCS reads with a coverage of 912, while absent with 0 DCS reads in all other biopsies with a coverage between 816 and 2,013 at that position. These data demonstrate that subclonal mutations in the cancer driver genes do occur frequently.

When we observed intratumor genetic heterogeneity by multiregion sequencing both at the copy number level and the mutation level, we wondered whether we could establish heterogeneous cell lines from multiregion biopsies of tumors. As different cell lines may have very different morphologies with respect to cell volume and shape, we focused on morphological distinction. We tested eight biopsies and noted in two cases cells with different morphology in culture. In one case we could not separate these by differential trypsinization. For the other case we could establish two distinct cell lines from one tumor biopsy. The two clones showed the same mutation in the 29 tested cancer driver genes, but were clearly distinct at the copy number level (Fig. 4a/4b). They also expressed other proteins as shown by immunostaining

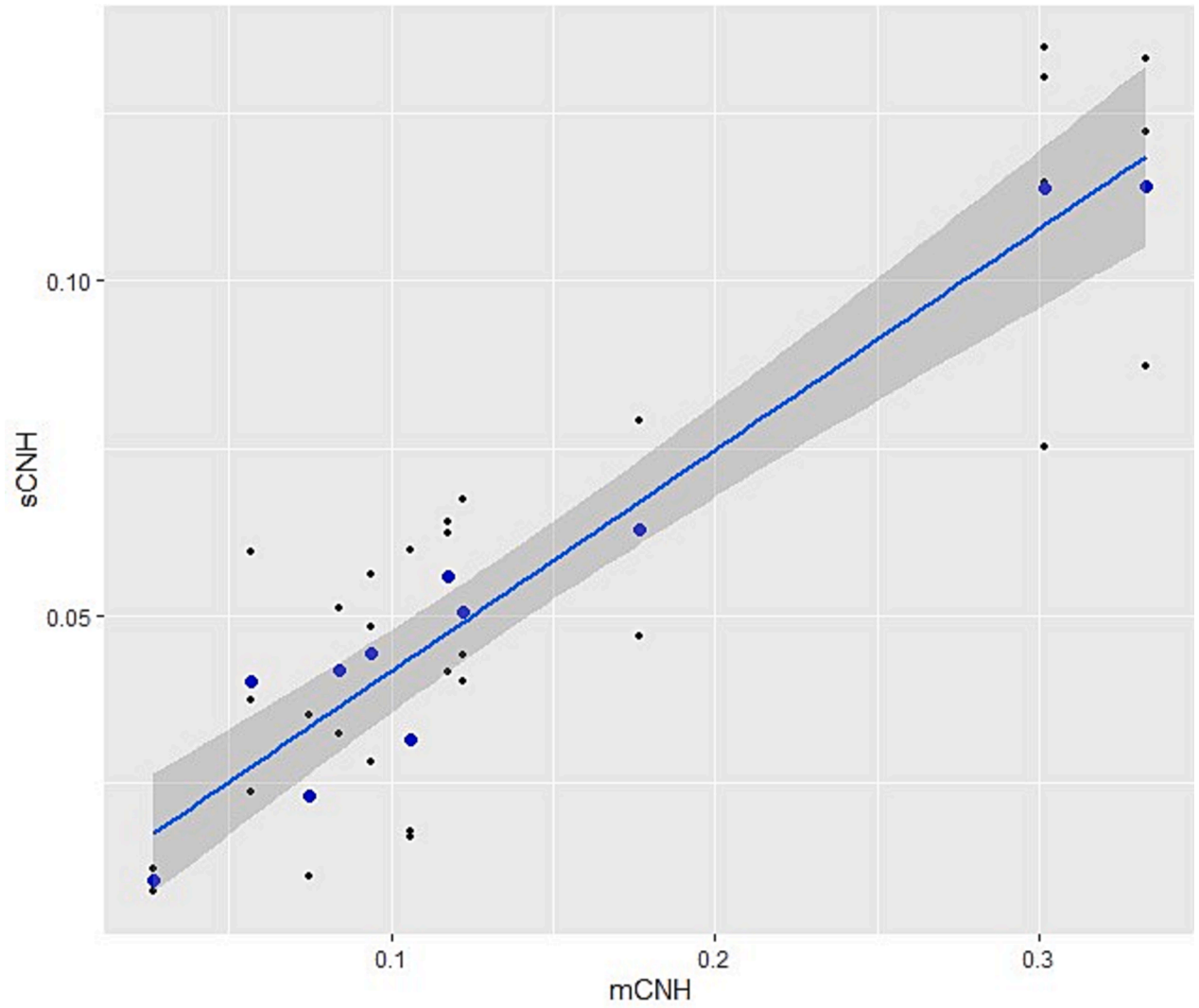

Fig. 2. (*continued*).

(Fig. 4c). Cell line A shows signs of epithelial-mesenchymal transition (EMT) with strong vimentin immunostaining and absence of CD44v6. Also, the difference in MCL1 inhibitor response between the lines is remarkable and amounts to one log difference of IC50 (Fig. 4d). Review of the histological slides of the tumor specimen did reveal differences determined by staining for vimentin and CD44v6, although this is somewhat blurred by the high background of vimentin staining in stromal fibroblasts (Fig. 4e).

Discussion

The observation that a certain percentage of relapses after CRT are genetically discordant, has been observed in three independent studies at different centers and forms a challenging problem for the future. The pathobiological mechanism of these genetically unrelated local relapses after RT/CRT remains at present unclear. There a multiple explanations possible including field cancerization and even completely independent origin as second primary tumors. Identification of the pathobiological mechanisms that cause development of LR will improve our understanding of this phenomenon and may point to prognostic relevance and better treatments. For definitive (C)RT also treatment-induced genetic changes and intratumor genetic heterogeneity might play a role, and these two instigating explanations were investigated in this study.

In previous studies it has been shown that radiation causes DNA damage such as single stranded and double stranded breaks, and also the relevance of DNA repair in radioresistance is well studied [15,23]. Alexandrov et al. reported that mutational signatures associated with chemotherapy, including cisplatin, and RT can be deduced by genome sequencing[14]. However, based on the experimental data in the xenograft models, it appears that treatment–induced genetic changes that turn into clonal driver mutations do not occur, and are an unlikely explanation for these seemingly genetically unrelated relapses.

As an alternative mechanism, we studied intratumoral heterogeneity by comparing CNAs and mutations between multiregion biopsies of one resection specimen. We could only study this in resection specimen of oral cancers, which are typically not treated by definitive (chemo) radiotherapy, but we assume that these data can be well extrapolated, although this should be proven in future prognostic studies. We demonstrated many differences between copy number profiles, and calculated a multisample CNH-score that varied between 0.027 and 0.333. A potential limitation of our study was that the number of biopsies per tumor was uneven, which might have impacted the calculations. However, when our multisample CNH score was compared to the single-sample CNH score previously described by van Dijk et al.[21], these correlate well. Perhaps unsurprisingly, copy number profiles strongly supported clonal relations between samples of the same tumor in all patients.

In contrast to CNAs, mutations can be very specifically called even at

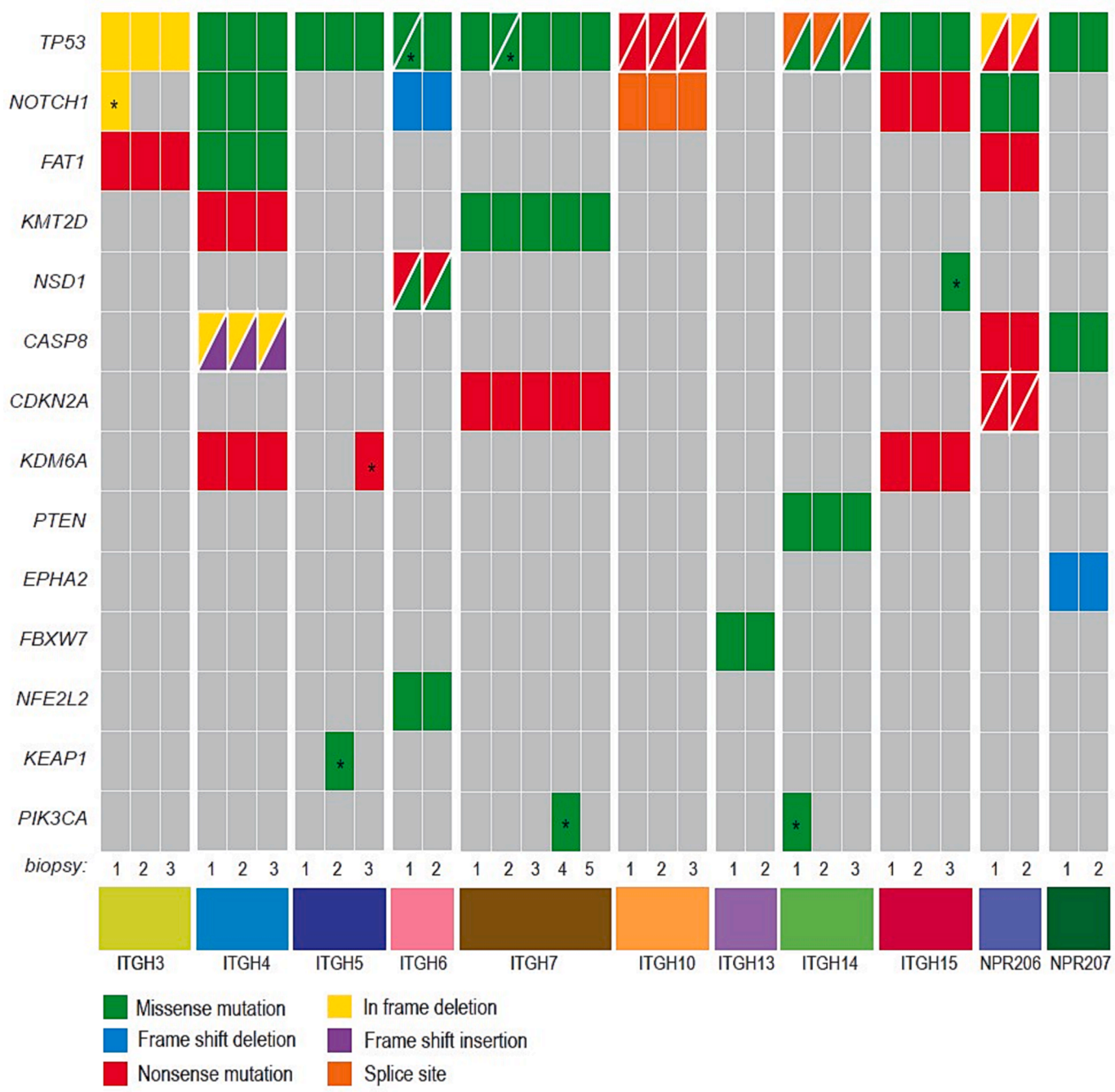

Fig. 3. Oncoplot of mutations in multiregion biopsies. The clonal mutations are depicted of all biopsies of all tumors. Patient ID is indicated below the plot in color code. The subclonal mutations are marked with (*) and determined by the DCS pipeline with a minimum of 3 variant reads and after exclusion of clonal variants and germline variants. Type of mutation is color coded. When two alleles are mutated they are indicated with triangles. Detailed data on the mutations are indicated in Supplementary Tables 2 and 3. Note that clonal mutations are always shared, but subclonal mutations in the same driver genes frequently occur.

lower abundance. Most cloncal mutations were identical but we found that 6 out of 11 tumors contained subclonal mutations in the HNSCC cancer driver genes. Importantly, this impacted the earliest cancer driver genes such as *TP53* as if these tumors are of multiclonal origin.

Future studies have to show whether genetic heterogeneity at the CNA level and cancer driver gene level as reported here, correlates with treatment response and outcome. Also the relevance for novel treatments such as immunotherapy, need to be addressed.

As indicated above, the presence of genetically distinct recurrences in HNSCCs also raises questions about the potential role of second primary tumors (SPT). Although this has not been observed for LRs after surgery, this might be different after definitive CRT. While our subsequent study focused on intratumor genetic heterogeneity as a potential explanation, the possibility of SPTs following treatment cannot be ignored. This is a relevant finding also in the broader context of protons versus photons.

In conclusion, seemingly genetically unrelated recurrences occur in 10–50 % of treated head and neck cancer patients after (C)RT. Treatment induction of DNA changes seems the most unlikely explanation for this phenomenon. Intratumor genetic heterogeneity and treatment-induced selection of specific subclones is a more likely explanation, although both field cancerization and independent clonal origin need to be considered.

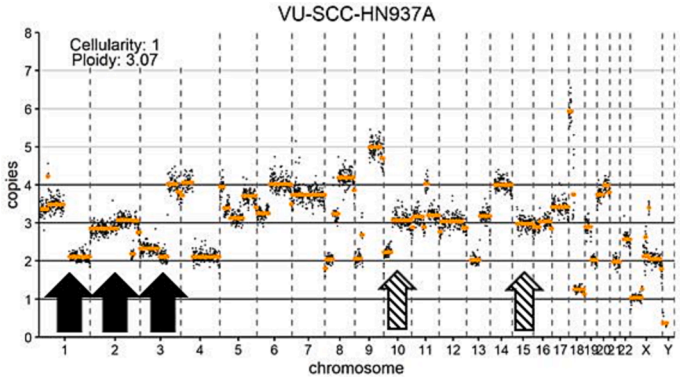

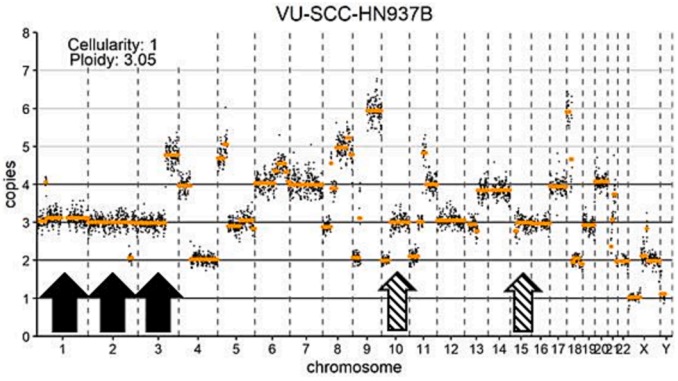

VU-SCC-HN937A

CHR	POS	GENE	REF	ALT	DP	AD	FREQ	CHANGE
Chr17	7577555	TP53	GC	AA	480	480	100%	p.C242F
Chr4	1.88E+08	FAT1	C	CATAT	350	350	100%	p.M194fs
Chr9	21971098	CDKN2A	C	CG	520	520	100%	p.R36fs

VU-SCC-HN937B

CHR	POS	GENE	REF	ALT	DP	AD	FREQ	CHANGE
Chr17	7577555	TP53	GC	AA	1654	1654	100%	p.C242F
Chr4	1.88E+08	FAT1	C	CATAT	878	878	100%	p.M194fs
Chr9	21971098	CDKN2A	C	CG	1026	1026	100%	p.R36fs

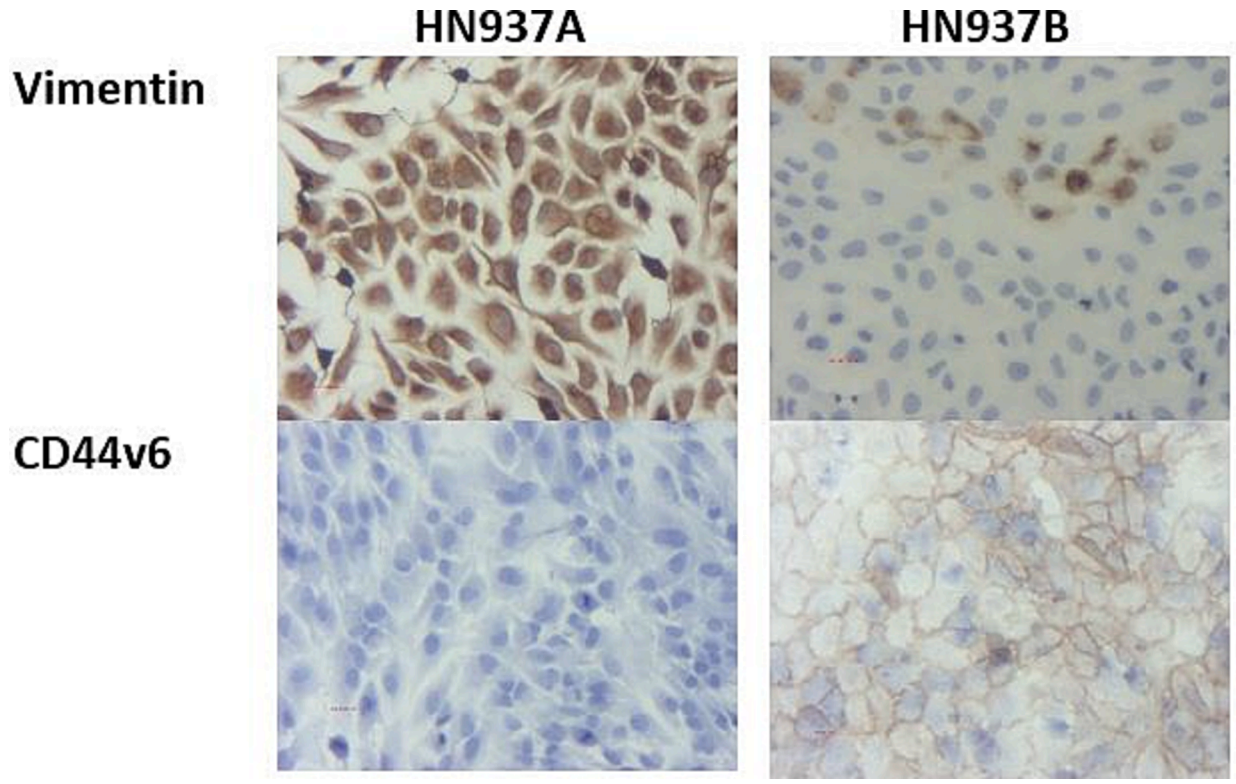

	drug			WEE-1	MCL-1
Cell line	CDDP	nutlin3a	illudinS	MK1775	S63845
VU-SCC-HN937A	8.97	27,4	9,31	0,36	6,36
VU-SCC-HN937B	2.10	22,3	17,3	0,12	0,71

Fig. 4. Molecular differences between cell lines VU-SCC-HN937A and VU-SCC-HN937B. Two cell lines were generated from one tumor biopsy. A) Copy number plots of HN937A and HN937B. Some differences are indicated with a closed arrow and some similarities are indicated with an open arrow. B) Table with detected variants in the cancer driver genes. C) Differences in expressed proteins determined by immunostaining, D) IC50 analysis of a panel of inhibitors. Note the major difference in MCLI inhibitor response. E) Differences determined by CD44v6 staining with U36 (left) and vimentin (right) indicated with an arrow.

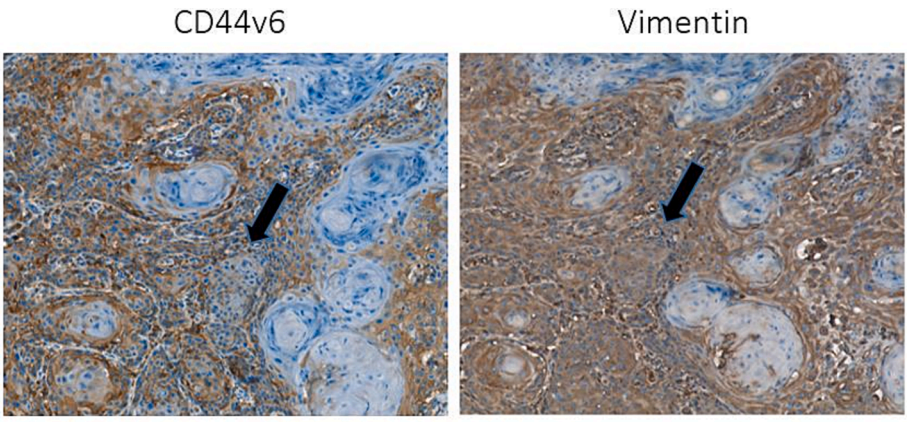

Fig. 4. (*continued*).

CRediT authorship contribution statement

A.S. Pierik: Investigation, Visualization, Formal analysis, Project administration. **J.B. Poell:** Software, Data curation, Resources, Formal analysis, Visualization, Writing – review & editing. **A. Brink:** Data curation, Formal analysis, Resources, Visualization, Writing – review & editing. **M. Stigter- van Walsum:** Resources, Visualization, Writing – review & editing. **R.H. de Roest:** Writing – review & editing. **T. Poli:** Resources, Writing – review & editing. **A. Yaromin:** Resources, Visualization, Writing – review & editing. **P. Lambin:** Resources, Writing – review & editing. **C.R. Leemans:** Writing – review & editing, Supervision. **R.H. Brakenhoff:** Writing – review & editing, Supervision, Conceptualization, Funding acquisition.

Declaration of competing interest

The authors declare that they have no known competing financial interests or personal relationships that could have appeared to influence the work reported in this paper.

Acknowledgement

The authors thank all participating individuals, prof. dr. E. Bloemena and dr. L. Peferoen for review of pathological slides. This study was funded by KWF kankerbestrijding (12079).

Data availability

Data and code that support the findings of this study are available on request from the corresponding author. The data cannot be made publicly available due to privacy or ethical restrictions.

Appendix A. Supplementary material

Supplementary data to this article can be found online at https://doi.org/10.1016/j.radonc.2024.110087.

References

[1] Siegel RL, Miller KD, Jemal A. Cancer statistics, 2019. CA Cancer J Clin 2019;69:7–34.
[2] Bray F, Ferlay J, Soerjomataram I, Siegel RL, Torre LA, Jemal A. Global cancer statistics 2018: GLOBOCAN estimates of incidence and mortality worldwide for 36 cancers in 185 countries. CA Cancer J Clin 2018;68:394–424.
[3] Leemans CR, Snijders PJF, Brakenhoff RH. The molecular landscape of head and neck cancer. Nat Rev Cancer 2018;18:269–82.
[4] Castellsagué X, Alemany L, Quer M, Halec G, Quirós B, Tous S, et al. HPV Involvement in Head and Neck Cancers: Comprehensive Assessment of Biomarkers in 3680 Patients. J Natl Cancer Inst. 2016;108(6):djv403.
[5] Leemans CR, Braakhuis BJM, Brakenhoff RH. The molecular biology of head and neck cancer. Nat Rev Cancer 2011;11:9–22.
[6] Rohde M, Rosenberg T, Pareek M, Nankivell P, Sharma N, Mehanna H, et al. Definition of locally recurrent head and neck squamous cell carcinoma: a systematic review and proposal for the Odense-Birmingham definition. Eur Arch Otorhinolaryngol 2020;277:1593–9.
[7] de Roest RH, van der Heijden M, Wesseling FWR, de Ruiter EJ, Heymans MW, Terhaard C, et al. Disease outcome and associated factors after definitive platinum based chemoradiotherapy for advanced stage HPV-negative head and neck cancer. Radiother Oncol 2022;175:112–21.
[8] Hedberg ML, Goh G, Chiosea SI, Bauman JE, Freilino ML, Zeng Y, et al. Genetic landscape of metastatic and recurrent head and neck squamous cell carcinoma. J Clin Invest 2016;126:1606.
[9] van Houten VM, Leemans CR, Kummer JA, Dijkstra J, Kuik DJ, van den Brekel MW, et al. Molecular diagnosis of surgical margins and local recurrence in head and neck cancer patients: a prospective study. Clin Cancer Res 2004;10:3614–20.
[10] Tabor MP, Brakenhoff RH, Ruijter-Schippers HJ, Kummer JA, Leemans CR, Braakhuis BJ. Genetically altered fields as origin of locally recurrent head and neck cancer: a retrospective study. Clin Cancer Res 2004;10:3607–13.
[11] Graveland AP, Golusinski PJ, Buijze M, Douma R, Sons N, Kuik DJ, et al. Loss of heterozygosity at 9p and p53 immunopositivity in surgical margins predict local relapse in head and neck squamous cell carcinoma. Int J Cancer 2011;128:1852–9.
[12] de Roest RH, Mes SW, Poell JB, Brink A, van de Wiel MA, Bloemena E, et al. Molecular characterization of locally relapsed head and neck cancer after concomitant chemoradiotherapy. Clin Cancer Res 2019;25:7256–65.
[13] Weber P, Künstner A, Hess J, Unger K, Marschner S, Idel C, et al. Therapy-related transcriptional subtypes in matched primary and recurrent head and neck cancer. Clin Cancer Res 2022;28:1038–52.
[14] Alexandrov LB, Kim J, Haradhvala NJ, Huang MN, Tian Ng AW, Wu Y, et al. The repertoire of mutational signatures in human cancer. Nature 2020;578:94–101.
[15] Kocakavuk E, Anderson KJ, Varn FS, Johnson KC, Amin SB, Sulman EP, et al. Radiotherapy is associated with a deletion signature that contributes to poor outcomes in patients with cancer. Nat Genet 2021;53:1088–96.
[16] Gerlinger M, Rowan AJ, Horswell S, Larkin J, Endesfelder D, Gronroos E, et al. Intratumor heterogeneity and branched evolution revealed by multiregion sequencing. N Engl J Med 2012;366:883–92.
[17] McGranahan N, Swanton C. Clonal heterogeneity and tumor evolution: Past, present, and the future. Cell 2017;168:613–28.
[18] Turajlic S, Sottoriva A, Graham T, Swanton C. Resolving genetic heterogeneity in cancer. Nat Rev Genet 2019;20:404–16.
[19] van Harten AM, de Boer DV, Martens-de Kemp SR, Buijze M, Ganzevles SH, Hunter KD, et al. Chemopreventive targeted treatment of head and neck precancer by Wee1 inhibition. Sci Rep 2020;10:2330.
[20] Schmitt MW, Fox EJ, Prindle MJ, Reid-Bayliss KS, True LD, Radich JP, et al. Sequencing small genomic targets with high efficiency and extreme accuracy. Nat Methods 2015;12:423–5.
[21] van Dijk E, van den Bosch T, Lenos KJ, El Makrini K, Nijman LE, van Essen HFB, et al. Chromosomal copy number heterogeneity predicts survival rates across cancers. Nat Commun 2021;12:3188.
[22] Comprehensive genomic characterization of head and neck squamous cell carcinomas. Nature. 2015;517(7536):576-82.
[23] Behjati S, Gundem G, Wedge DC, Roberts ND, Tarpey PS, Cooke SL, et al. Mutational signatures of ionizing radiation in second malignancies. Nat Commun 2016;7:12605.